

SCATTERING MULTI-CONNECTIVITY ESTIMATION FOR INDOOR MMWAVE SMALL CELLS UNDER LIMITED TRAINING STEPS

Hung-Yi Cheng, Ching-Chun Liao, and An-Yeu (Andy) Wu, Fellow, IEEE

Graduate Institute of Electronics Engineering, National Taiwan University, Taipei, 106, Taiwan, R.O.C.
 {woody, cliao}@access.ee.ntu.edu.tw, andywu@ntu.edu.tw

ABSTRACT

Multi-connectivity, connections among multiple small cells (SCs) simultaneous, is used to be a promising solution to achieve high reliability in indoor millimeter-wave (mmWave) networks. This work further improves the multi-connectivity estimation under scenarios with strictly-limited training steps. To quickly estimate multiple links connected to different SCs, we propose a novel scattering multi-beam codebook (SMBC). Then, we develop a scattering multi-connectivity estimation (SMCE) measuring effective possible links instead of all possible links. From our simulation results, our method can complete multi-connectivity in only 20% of the training steps in the uplink exhaustive measurement (UEM).

Index Terms—5G communications, indoor mmWave, low latency, multi-connectivity, high reliability.

1. INTRODUCTION

The upcoming fifth generation wireless communication standard (5G) supporting low latency creates new indoor business demands, such as Industry 4.0, the factory of the future [1]. Under tight timing constraints, some applications further require ultra-reliable communication, for instance mission-critical controls, while others need to involve high-throughput transmission, for instance augmented reality (AR) [1], [2]. Regarding various resource-hungry services, it is very challenging to fulfill the stringent timing requirements. To address these critical issues, currently, multi-connectivity techniques emerge, where user equipment (UE) can be simultaneously connected to several small cells (SCs) [3]-[6].

Multi-connectivity [3] presents much stronger robustness than a single connection to the strongest cell. However, multi-link estimation of multi-connectivity is more complicated in mmWave due to its highly directional channel paths. Under low-latency requirements, training time is even more limited [7]. With stringent timing constraints, uplink exhaustive measurement (UEM) [4], [5], which is capable of measuring all possible links to all SCs, would fail because of exhaustion of the training time. Fortunately, in an indoor mmWave environment, path loss is more favorable. More possible links exist. Hence, by exploiting a subset of the possible links, a UE can complete multi-connectivity strategies.

In this paper, we take the advantage of the multi-beam effect in our previous work [8], progressive multi-beam estimation (PMBE), and further concentrate on such an indoor low-latency mmWave scenario. A fast multi-link estimation of multi-

TABLE 1. COMPARISON WITH RELATED WORKS.

	Multi-Link Estimation	Multi-SC Detection	Multi-Best Process	Multi-Connectivity Quality under strictly-limited training time
UEM [4][5]	⊙	⊙		Highest quality, but fails under strictly-limited training time
PMBE [8]	⊙		⊙	Fast multi-link estimation, but fails with multiple APs connection
Proposed SMCE	⊙	⊙	⊙	Highest quality even under strictly-limited training time

connectivity is developed. Our method aims to measure as many links as possible in a limited training time instead of all possible links to all SCs. Multi-connectivity is rapidly established. Moreover, multi-connectivity quality keeps enhanced until the training time expires. The main contributions are summarized as follows:

- 1) *Scattering Multi-Beam Codebook*: to quickly measure more possible links, we propose a novel scattering multi-beam codebook (SMBC). Each probing vector of this codebook forms a scattering multi-beam pattern, and simultaneously probes different spatial directions, so as to enhance the multi-link estimation.
- 2) *Uplink Multi-SC Measurement*: we adopt an uplink channel estimation so that each probing vector on the UE side can probe all channel to all SCs.
- 3) *Three Multi-Best Processes*: by taking the advantage of multi-beam effect of [8], we propose three multi-best processes and develop a scattering multi-connectivity estimation (SMCE). This method concurrently measures subsets of all possible links to all SCs, thereby reducing the required training time. The comparison with the related works is listed in **Table 1**.

The remainder of the paper is organized as follows. In Section 2, we review the background of the related multi-link estimation. Section 3 presents the proposed scattering multi-connectivity estimation. Section 4 gives simulation results and Section 5 concludes this paper.

2. NOTATIONS AND RELATED WORK

2.1. Notations

We use the following notations for algorithm development. \mathbf{A} is a matrix, \mathbf{a} is a vector and a is a scalar. $\mathbf{a}[l]$ is the l -th element of the vector \mathbf{a} . $|\mathbf{A}|$ is the determinant of \mathbf{A} . $\mathcal{CN}(\mathbf{a}, \mathbf{A})$ is a complex Gaussian vector with mean vector \mathbf{a} and covariance matrix \mathbf{A} . $\mathbf{0}$ is a zero vector. \mathbf{I}_N denotes an $N \times N$ identity

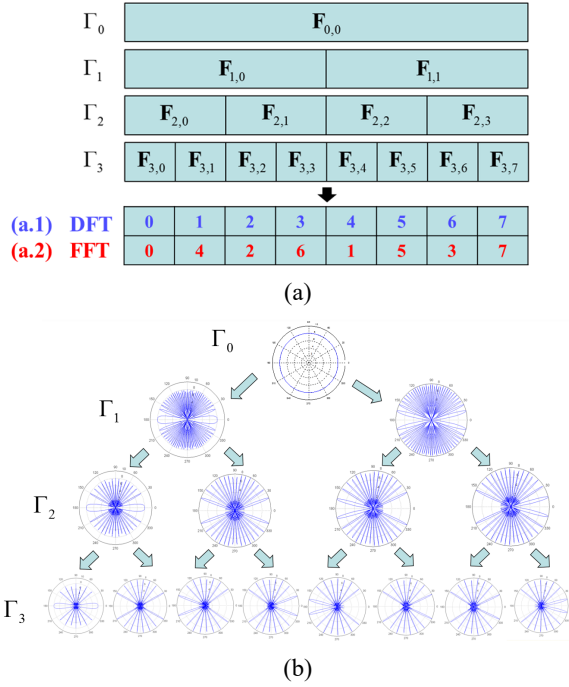


Fig. 1. Proposed codebook design. (a) A hierarchical codebook structure with partition parameter $R=2$ and 8 antennas. (b) Beam pattern of the SMBC structure with 64 antennas. All elements of our codebook are multi-beam probing vectors.

matrix. The superscripts H and -1 denote the conjugate transpose and inverse, respectively.

2.2. Uplink Exhaustive Measurement (UEM)

A mmWave UE and SCs utilize directional phase arrays for transmission. We let N_{UE} and N_{SC} be the number of directions at the UE and each SC, respectively. Therefore, UEM requires at least $N_{UE} \times N_{SC}$ training steps. Assume all devices can communicate via N_s independent data streams, and the UE and each SC are equipped with N_t transmit and N_r receive antennas, respectively. Hence, the received uplink signal at the m -th SC can be expressed as

$$\mathbf{y}^{(m)} = \sqrt{\rho} [\mathbf{Z}_{SC}^m]^H \mathbf{H}_m \mathbf{F}_{UE} \mathbf{s}_m + [\mathbf{Z}_{SC}^m]^H \mathbf{n}. \quad (1)$$

\mathbf{s}_m is the N_s -dimensional symbol vector, $\mathbf{Z}_{SC}^m \in \mathbb{C}^{N_r \times N_s}$ is the m -th SC combiner, and $\mathbf{F}_{UE} \in \mathbb{C}^{N_t \times N_s}$ is a UE precoder. ρ denotes an average signal power of the received signal. $\mathbf{n} \in \mathbb{C}^{N_r \times 1}$, is a noise vector modeled as $\mathcal{CN}(\mathbf{0}, \mathbf{I}_{N_r})$. $\mathbf{H}_m \in \mathbb{C}^{N_r \times N_t}$ is a complex MIMO channel between the m -th SC and the UE.

3. PROPOSED SCATTERING MULTI-CONNECTIVITY ESTIMATION ALGORITHM

For a single multi-path mmWave channel, we have proposed a progressive multi-beam estimation (PMBE) [8]. The PMBE

tends to iteratively estimate multiple channel gains, thus leading to a progressive multi-beam effect. Because of this multi-beam effect, high spectral efficiency can be achieved in a short training time. We take the advantage of the multi-beam effect and propose a novel fast multi-link estimation for an indoor multi-connectivity mmWave scenario with latency constraints.

3.1. Hierarchical Codebook Structure

Fig. 1(a.1) demonstrates a Discrete Fourier Transform (DFT)-based codebook structure of a transmitter used in PMBE. This hierarchical DFT-based codebook consists of $S_x + 1$ levels ($S_x = \log_M N_t$). Γ_s is the set of all precoding vectors at the level s , $s = 0, 1, \dots, S_x$. Each probing vector at the highest level S_x is designed by a column of the N_t -point DFT matrix in increasing order. At the level s , the probing vector $\mathbf{F}_{s,q}$ is designed as

$$\mathbf{F}_{s,q} = \frac{1}{R} \sum_{r=1}^R \mathbf{F}_{s+1, R(q-1)+r}, \quad (2)$$

where R is a design parameter for codebook partitioning, and q refers to a probing index of level s .

3.2. Scattering Multi-beam Codebook (SMBC)

To quickly estimate multiple links to different SCs, we propose a novel scattering multi-beam codebook (SMBC). First, we reorder the index of the N_t -point DFT matrix (Fig. 1(a.1)) into its bit-reversal order, seen as a Fast Fourier Transform (FFT) order (Fig. 1(a.2)). That is, each probing vector at the level S_x is set by one column of the N_t -point DFT matrix in bit-reversal order (FFT order). Next, we group this permutation into a hierarchical codebook structure. Fig. 1(b) shows the scattering multi-beam patterns of this codebook. In traditional communication, FFT is used to separate a time domain signal into different frequency components. In our scheme, based on FFT structure, SMBC is used to separate a transmitting or incoming signal into different spatial directions, so as to accelerate the multi-link estimation. Similarly, all the described techniques equally apply to the combiners.

3.3. Scattering Multi-Connectivity Estimation (SMCE)

Fig. 2 shows the procedure of the proposed SMCE. First, the UE and each SC have their hierarchical codebook structure of SMBC. Based on these codebooks, we start an uplink multi-SC measurement. Then, we utilize three different multi-best (k -best) processes to select effective links to different SCs. Hence, our algorithm can rapidly respond to multiple possible links in a short training time. Meanwhile, multi-connectivity quality keeps enhanced with another iteration. In the following, we depict step (a) to (g) from Fig. 2 in detail.

- At each level s , the UE index set and the m -th SC index set are denoted as $I_{(s)}$ and $J_{(s)}^m$, respectively, where $m = 1, 2, \dots, M$. M is the number of SCs. In the initial stage, we set the level $s = S_{init}$ ($S_{init} < S_x$) for the UE and all SC codebooks. Then, in the level S_{init} , we set

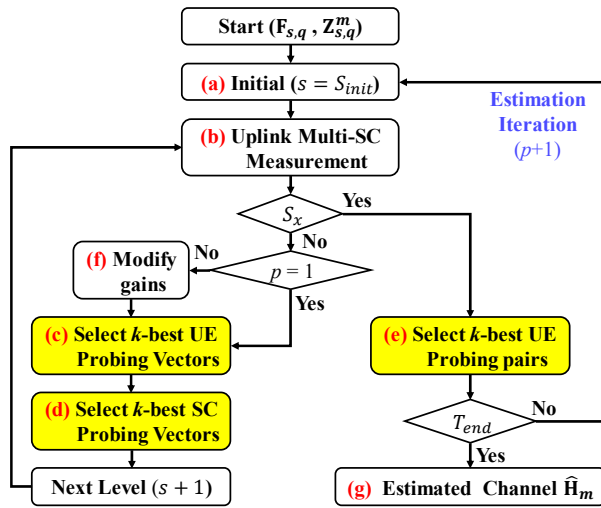


Fig. 2. The procedure of the SMCE. Yellow blocks are detail functions belong to three different multi-best processes. T_{end} means the end of the training time. Parameter p represents the number of iterations.

$$\begin{aligned} I_{(S_{init})} &= \{0, 1, 2, \dots, 2^{S_{init}} - 1\}, \text{ and} \\ J_{(S_{init})}^m &= \{0, 1, 2, \dots, 2^{S_{init}} - 1\}, \end{aligned} \quad (3)$$

which comprise all probing indexes in the level S_{init} of the UE and the m -th SC code books, respectively.

- (b) At the level s , by adaptively switching the UE and the m -th SC probing vectors whose probing index belongs to $I_{(s)}$ and $J_{(s)}^m$, respectively, the m -th SC measures several gains. By setting $\mathbf{s}_m = [1 \ 0 \ \dots \ 0]_{N_s}$, all estimated gains of all SCs can be expressed as

$$\begin{aligned} \alpha_{i,j}^{(s,m)} &= \sqrt{\rho} [\mathbf{z}_{s,j}^m]^H \mathbf{H}_m \mathbf{F}_{s,i} + [\mathbf{z}_{s,j}^m]^H \mathbf{n}, \\ \text{s. t. } \forall i &\in I_{(s)}, j \in J_{(s)}^m, m \in \{1, 2, \dots, M\}. \end{aligned} \quad (4)$$

- (c) After comparing all estimated gains, the UE determines the k -best UE probing gains by

$$\begin{aligned} (\alpha_{i_{t_1}, j_{t_1}}^{(s, m_1)}, \alpha_{i_{t_2}, j_{t_2}}^{(s, m_2)}, \dots, \alpha_{i_{t_k}, j_{t_k}}^{(s, m_k)}) &= \max_{i,j,m} k(\alpha_{i,j}^{(s,m)}) \\ \text{s. t. } \forall i &\in I_{(s)}, j \in J_{(s)}^m, m \in \{1, 2, \dots, M\}, \end{aligned} \quad (5)$$

where function $\max_k(X)$ returns k maximum values of a set X . From (5), the k -best UE probing indexes are i_{t_1}, i_{t_2}, \dots , and i_{t_k} . According to (2), each probing vector is divided into R probing vectors at the next level. Hence, we design the UE index set of next level as

$$I_{(s+1)} = \left\{ R(i-1) + r \mid \begin{array}{l} i \in \{i_{t_1}, i_{t_2}, \dots, i_{t_k}\}, \\ r \in \{1, 2, \dots, R\} \end{array} \right\}. \quad (6)$$

- (d) On the other side, the m -th SC compares its estimated gains belonging to i_{t_1}, i_{t_2}, \dots , and i_{t_k} . It determines the k -best probing gains by

$$\begin{aligned} (\alpha_{i_{r_1}, j_{r_1}}^{(s,m)}, \alpha_{i_{r_2}, j_{r_2}}^{(s,m)}, \dots, \alpha_{i_{r_k}, j_{r_k}}^{(s,m)}) &= \max_{i,j} k(\alpha_{i,j}^{(s,m)}) \\ \text{s. t. } \forall i &\in \{i_{t_1}, i_{t_2}, \dots, i_{t_k}\}, j \in J_{(s)}^m. \end{aligned} \quad (7)$$

Therefore, the k -best probing indexes of the m -th SC are $j_{r_1}^m, j_{r_2}^m, \dots$, and $j_{r_k}^m$. Similarly, we design the m -th SC index set of next level as

$$J_{(s+1)}^m = \left\{ R(j-1) + r \mid \begin{array}{l} j \in \{j_{r_1}^m, j_{r_2}^m, \dots, j_{r_k}^m\}, \\ r \in \{1, 2, \dots, R\} \end{array} \right\}. \quad (8)$$

Next, our algorithm shifts to the next level. Based on these index sets of the level $s+1$, we perform the uplink multi-SC measurement again from step (b), and proceed with the k -best processes until the level S_x is reached.

- (e) As S_x is reached, the m -th SC compares its estimated gains and determines the k -best probing pairs by:

$$\begin{aligned} (\alpha_{i_1^m, j_1^m}^{(S_x, m)}, \alpha_{i_2^m, j_2^m}^{(S_x, m)}, \dots, \alpha_{i_k^m, j_k^m}^{(S_x, m)}) &= \max_{i,j} k(\alpha_{i,j}^{(S_x, m)}) \\ \text{s. t. } \forall i &\in I_{(S_x)}, j \in J_{(S_x)}^m. \end{aligned} \quad (9)$$

From (9), the m -th SC stores k UE probing indexes, k m -th SC probing indexes, and k estimated gains into its vectors, \mathbf{i}_p^m , \mathbf{j}_p^m , and \mathbf{a}_p^m , respectively as follows:

$$\begin{aligned} \mathbf{i}_p^m &= [i_{p-1}^m, i_1^m, i_2^m, \dots, i_k^m], \\ \mathbf{j}_p^m &= [j_{p-1}^m, j_1^m, j_2^m, \dots, j_k^m], \\ \mathbf{a}_p^m &= [a_{p-1}^m, \alpha_{i_1, j_1}^{(S_x, m)}, \alpha_{i_2, j_2}^{(S_x, m)}, \dots, \alpha_{i_k, j_k}^{(S_x, m)}]. \end{aligned} \quad (10)$$

The parameter p represents the number of the iteration. $\mathbf{i}_0^m, \mathbf{j}_0^m$ and \mathbf{a}_0^m are empty vectors. If training time is still available, we iterate these k -best processes from step (a).

- (f) After step (b) in the following iterations, each estimated gain of the m -th SC should be modified by removing the contributions of the previously estimated gains, that is,

$$g_m = \sum_{l=1}^{(p-1)k} \mathbf{F}_{s,i}^T \mathbf{F}_{s_x, i_p^m}^* [l] [\mathbf{z}_{s,j}^m]^H \mathbf{z}_{s_x, j_p^m}^m [l], \text{ and} \quad (11)$$

$$\alpha_{i,j}^{(s,m)} = \alpha_{i,j}^{(s,m)} - g_m * \alpha_{i,j}^{(s,m)}. \quad (12)$$

- (g) This iterative procedure is executed until training time expires. Finally, the m -th estimated mmWave channel can be reconstructed as

$$\hat{\mathbf{H}}_m = \sum_{l=1}^{pk} \mathbf{a}_p^m [l] [\mathbf{z}_{s_x, i_p^m}^m [l]] [\mathbf{F}_{s_x, i_p^m}^m [l]]^H \quad (13)$$

To verify the effect of the SMBC-based SMCE, we further design a DFT-based SMCE as a benchmark by replacing the SMBC in the SMCE to the DFT-based codebooks.

4. SIMULATION RESULTS

For the following simulations, the m -th mmWave channel based on the Saleh Valenzuela model can be expressed as

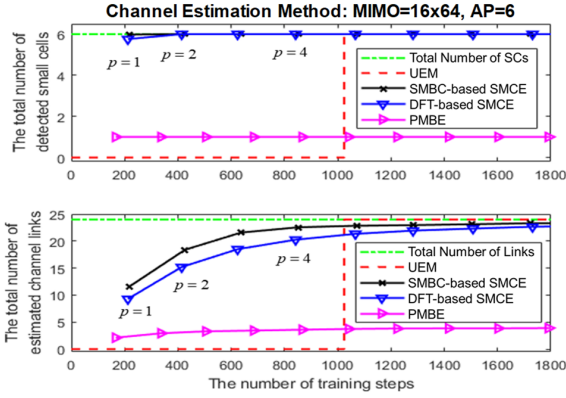


Fig. 3. The total number of detected SCs and estimated channel links in different training steps.

$$\mathbf{H}_m = \sqrt{\frac{N_t N_r}{L}} \sum_{l=1}^L \alpha_l \mathbf{a}_r(\varphi_l^r) \mathbf{a}_t^H(\varphi_l^t), \quad (14)$$

where L is the number of channel paths. φ_l^t and φ_l^r correspond to the azimuth angles of departure and arrival of the l -th cluster, respectively. α_l is a complex standard Gaussian gain of the l -th links. An N -elements uniform linear array (ULA) is written as

$$\mathbf{a}(\varphi) = \frac{1}{\sqrt{N}} \left[\mathbf{1}, e^{j\frac{2\pi}{\lambda} d \sin(\varphi)}, \dots, e^{j(N-1)\frac{2\pi}{\lambda} d \sin(\varphi)} \right]^T, \quad (15)$$

where d and λ stand for the antenna spacing and the signal wavelength, respectively. We assume channel, codebook and hybrid beamforming parameters as $L = 4, R = 2, N_t = N_{SC} = 16, N_r = N_{UE} = 64, S_{init} = 2, N_{RF}^t = 4, N_{RF}^r = 8,$ and $N_s = k = 4.$ N_{RF}^t and N_{RF}^r are the number of UE and SC RF chains, respectively. The number of analog quantization bits is 6. The number of SCs is 6. All curves are averaged over 100 channel realizations.

4.1. Multi-SC Detection and Multi-link Estimation

We perform singular value decomposition (SVD) on the estimator $\hat{\mathbf{H}}_m$, and only compare r_m eigenbeam pairs whose eigenvalues are larger than 0.1 times the average signal power. Due to the existence of the eigenbeam pairs, the m -th SC is detected, and available for maintaining r_m possible links to the UE. Therefore, the number of possible links, or estimated channel links, of the m -th SC is defined as $r_m, r_m \leq L$.

Fig. 3 demonstrates the three main features of the proposed SMBC-based SMCE. First, by the scattering multi-beam codebooks, the SMBC-based SMCE establishes more possible channel links to all detected SCs than the DFT-based SMCE does. Secondly, as shown in the upper diagram of Fig. 3, due to the uplink measurement, the UE can connect to all SCs simultaneously by the SMBC-based SMCE while by PMBE it can only connect to one SC. Thirdly, as shown in the lower diagram of Fig. 3, due to the multi-best processes, the SMBC-based SMCE estimates as many links as possible instead of all

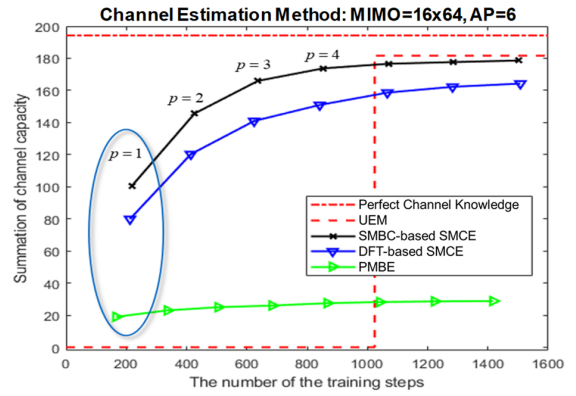


Fig. 4. Comparison of channel capacity vs. number of training steps. The blue circle is under strictly-limited training time.

possible links to all SCs. Hence, based on FFT structure, the SMBC-based SMCE only takes 20% of the training steps in UEM to achieve multi-connectivity.

4.2. Multi-Connectivity Quality vs. Training Steps

The multi-connectivity quality relates not only to the number of possible estimated links but also to the received capacity gain or diversity gain. We evaluate the multi-connectivity quality by summing up channel capacity of all estimated links. The summation can be expressed as follows:

$$C_{\text{sum}} = \sum_{m=0}^M \log_2 \left| I_{N_s} + \frac{\rho}{R_m} [Z_{SC}^m]^H \mathbf{H}_m \mathbf{F}_{UE}^m \times [\mathbf{F}_{UE}^m]^H \mathbf{H}_m Z_{SC}^m \right|, \quad (16)$$

where $R_m = N_s [Z_{SC}^m]^H \mathbf{F}_{UE}^m [\mathbf{F}_{UE}^m]^H Z_{SC}^m$ represents the noise covariance matrix. The hybrid beamforming parameters ($\mathbf{F}_{UE}^m, Z_{SC}^m$) are designed by the eigenbeam pairs of $\hat{\mathbf{H}}_m$ from Algorithm 1 of [9].

Fig. 4 shows, under strictly-limited training time, how our method provides better multi-connectivity quality compared to UEM and PMBE. As the number of the training step increases, the multi-connectivity quality of the SMBC-based SMCE remains superior and approaches that of UEM. Similarly, because of using the multi-beam probing vectors, the SMBC-based SMCE always has a better performance than the DFT-based SMCE.

5. CONCLUSION

This work concentrates on a multi-connectivity channel estimation under strictly-limited training steps. We propose the SMBC-based SMCE. This algorithm estimates as many links as possible in a limited training time instead of all possible links to all SCs. From the simulations, our method achieves multi-connectivity in only 20% of the training steps in UEM. Hence, the SMBC-based SMCE is quite efficient for indoor mmWave small cells under limited training steps.

6. REFERENCES

- [1] M. A. Lema *et al.*, "Business Case and Technology Analysis for 5G Low Latency Applications," *IEEE Access*, vol. 5, pp. 5917-5935, 2017.
- [2] B. Holfeld *et al.*, "Wireless Communication for Factory Automation: an opportunity for LTE and 5G systems," in *IEEE Communications Magazine*, vol. 54, no. 6, pp. 36-43, June 2016.
- [3] D. Ohmann, A. Awada, I. Viering, M. Simsek and G. P. Fettweis, "Impact of Mobility on the Reliability Performance of 5G Multi-Connectivity Architectures," *2017 IEEE Wireless Communications and Networking Conference (WCNC)*, San Francisco, CA, 2017, pp. 1-6.
- [4] M. Giordani, M. Mezzavilla, S. Rangan and M. Zorzi, "Multi-connectivity in 5G MmWave Cellular Networks," *2016 Mediterranean Ad Hoc Networking Workshop (Med-Hoc-Net)*, Vilanova i la Geltru, 2016, pp. 1-7.
- [5] M. Polese, M. Giordani, M. Mezzavilla, S. Rangan and M. Zorzi, "Improved Handover Through Dual Connectivity in 5G mmWave Mobile Networks," in *IEEE Journal on Selected Areas in Communications*, vol. 35, no. 9, pp. 2069-2084, Sept. 2017.
- [6] V. Petrov *et al.*, "Dynamic Multi-connectivity Performance in Ultra-dense Urban Mmwave Deployments," *IEEE Journal on Selected Areas in Communications*, vol. 35, pp. 2038-2055, September 2017.
- [7] R. Ford, M. Zhang, M. Mezzavilla, S. Dutta, S. Rangan and M. Zorzi, "Achieving Ultra-Low Latency in 5G Millimeter Wave Cellular Networks," in *IEEE Communications Magazine*, vol. 55, no. 3, pp. 196-203, March 2017.
- [8] H. Y. Cheng, C. C. Liao and A. Y. Wu, "Progressive Channel Estimation for Ultra-low Latency Millimeter-wave Communications," *2016 IEEE Global Conference on Signal and Information Processing (GlobalSIP)*, Washington, DC, 2016, pp. 610-614.
- [9] O. E. Ayach, S. Rajagopal, S. Abu-Surra, Z. Pi, and Jr. R.W. Heath, "Spatially Sparse Precoding in Millimeter Wave MIMO Systems," *IEEE Trans. on Wireless Commun.*, vol.13, no.3, pp.1499-1513, March 2014.